

# Effects of temperature and r.f. power sputtering on electrical and optical properties of $\text{SnO}_2$

Saad Hamzaoui\*, Mohamed Adnane

*Laboratoire de Microscopie Électronique, University of Sciences and Technology of Oran, BP1505 El Mnaouar, Oran, Algeria*

---

## Abstract

Electrical and optical properties of  $\text{SnO}_2$ , which is a photovoltaic material for solar energy conversion to electricity, have been investigated. Semi-conducting  $\text{SnO}_2$  has been grown by r.f. sputtering. We report the influence of process variables, such as substrate temperature and r.f. power. The film resistivity decreases with increasing temperature, but rises with increasing r.f. power: these can be related to crystallite size and the film orientation respectively. From the optical measurements, we deduce a variation of band-gap energy with substrate temperature. We show that the substrate temperature has a subsequent influence on the electrical and optical properties of this material. © 1999 Elsevier Science Ltd. All rights reserved.

---

## 1. Introduction

For some years, important developments have been achieved with respect to thin films of semi-conductor transparent oxides, notably due to their remarkable optical and electrical properties. In particular, ITO and ZnO films are competitive because of their abundance in nature and its relatively low cost.

The tin-oxide thin film is a degenerate n-type semi-conductor with a large band-gap of  $3.6 \text{ eV} < E_g < 4.0 \text{ eV}$ ; thus it has a strong transmission in the visible range ( $0.4\text{--}0.8 \mu\text{m}$ ) and a high absorption coefficient in the UV range ( $104\text{--}105 \text{ cm}^{-1}$ ).

Several authors [1,2] have studied  $\text{SnO}_2$  and shown that it has a weak resistance when its constituents are not in stoichiometric proportions, such that  $\text{SnO}_{2-x}$ ,  $x < 1$ . Its electrical resistivity can vary by several orders of magnitude following according to the deposition technique adopted. For the utilisation of  $\text{SnO}_2$  in photovoltaic applications, one needs to have specimens with weak resistivity values. It resists chemical attack, its adhesion to glass is very great [2]. Tin oxide crystallises in a

---

\* Corresponding author. Tel.: +213-6-454-368; fax: +213-6-421-581.

E-mail address: s\_hamzaoui@yahoo.com (S. Hamzaoui).

tetragonal rutilated structure, when it is deposited under optimal conditions, which allows it to have a weak shear resistance thereby giving it weak losses by Joule dissipation across electrical contacts.

To improve  $\text{SnO}_2$  films, one could employ r.f. sputtering, vapour deposition (C.V.D.) or spraying. The aim is to improve its photovoltaic properties. In the case of  $\text{SnO}_2$ , as for other metallic oxide drivers, an excess of tin or a deficit of oxygen contributes to the improvement of its properties. Annealing, and the doping by Sb, F, P or In are means for achieving these improvements.

Studies made on the evolution of tin-oxide films, prepared by r.f. sputtering, have revealed that substrate temperature, r.f. power, pressure and gas debit (e.g. argon/oxygen quotient) have considerable effects on the optical and electrical properties. The growth can be random or preferential. For solar cells, the  $\text{SnO}_2$  has been used in different forms: e.g. with a transparent conductive window such as a  $\text{Si:H/SnO}_2/\text{glass}$  or  $\text{MOS:SnO}_2/\text{SiO}_2/\text{Si(n)}$ .

## 2. Experimental details

Thin  $\text{SnO}_2$  films have been prepared by r.f. sputtering: a target of 8 cm diameter has been sintered with 99.99% pure  $\text{SnO}_2$  powder.

The films are deposited in a high-purity argon atmosphere; an approximately  $2 \times 10^{-5}$  torr vacuum being obtained before introducing the argon gas. The working pressure and the target substrate distance were respectively 25 mTorr and 5 cm. A Corning glass substrate was used.

In the first stage, the power was maintained at 150 W, for a deposition time of 60 min, and the substrate temperature could be varied from 50 to 350°C.

In the second stage, the temperature was fixed at 300°C, whereas the power was varied from 50 to 200 W in proportion to the time in order to always achieve the same film thickness.

The resistivity has been obtained at room temperature according to the Valdes conditions [3] using four equidistant and aligned probes.

The average transmission in the U.V. and visible ranges has been measured using a unique beam spectrophotometer.

The crystallographic structure of the film is examined by X-ray diffraction. The crystallite sizes were observed via a scanning electron-microscope. Using the Mani-facier [4] and Tauc [5] models, we have deduced the optical thickness, the average transmission, the absorption coefficient and the optical band-gap.

## 3. Results and discussions

### 3.1. Films crystallographic properties

Electrical properties of the films depend on crystallographic structure. To evaluate the effects of substrate temperature and power on the opto-electrical properties, we

have examined the deposited films by X-rays. Most of the films have a preferential orientation along the (101) axis. The orientation becomes random for powers exceeding 100 W. Other information can be extracted from these spectra, especially regarding the crystallite size, which can be estimated by the Sherrer Bragg relationship of  $[D_{hkl}] = 0.94\lambda/B\cos\theta_B$  where  $\lambda$  is the length of wave of the furrow,  $\text{Cu(K)} = 1.54 \text{ \AA}$ ,  $B$  being the width at middle height of the pic and  $\theta_B$  the Bragg angle.

Figs. 1 and 2 show the evolution of average size according to the temperature substrate and r.f. power: these have a net effect on the crystallite size, which increases from 40 to 110 nm.

### 3.2. Electrical properties

Fig. 3 shows the variation of the resistivity according to the substrate temperature: the resistivity decreases with the substrate temperature until  $250^\circ\text{C}$  at which temperature it tends to stabilise. The resistivity is dictated by the concentration of the carriers, the microstructure of the layer and the number of defects. The increase of

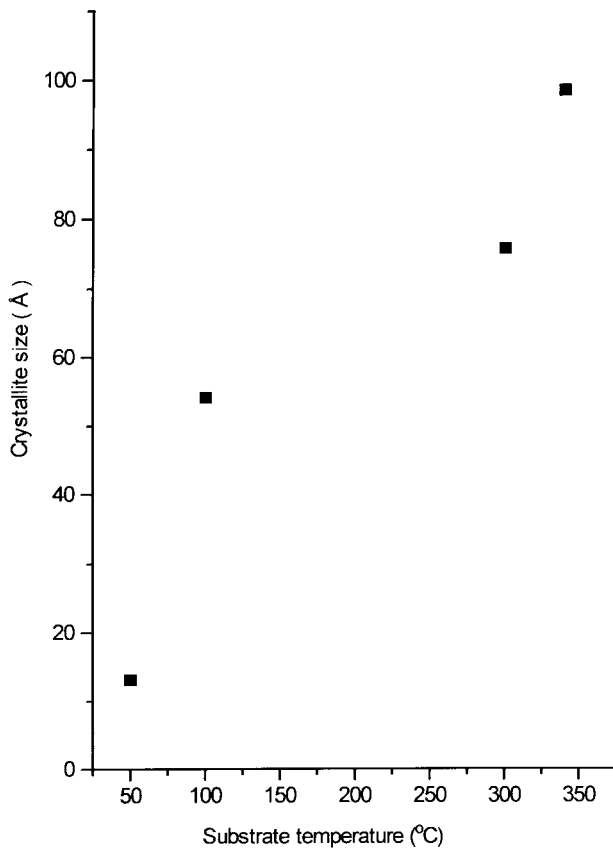


Fig. 1. Crystallite size of  $\text{SnO}_2$  as a function of substrate temperature.

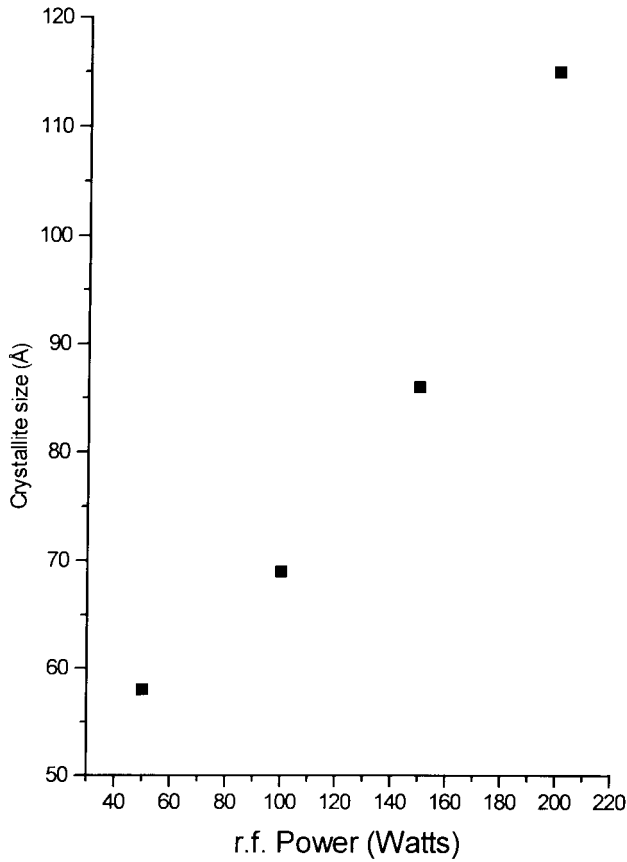


Fig. 2. Crystallite size of SnO<sub>2</sub> as a function of r.f. power.

the resistivity according to the r.f. power cannot be explained by the increase of the grain size, but by the poor orientation at high powers (Fig. 4).

### 3.3. Optical properties

The optical layer transmission ( $T_{\text{mes}}$ ) is defined by

$$T_{\text{mes}} = T/T_s \quad (1)$$

where  $T$  is the transmission of the system film-substrate, and  $T_s$  is the transmission of the substrate only [6].

### 3.4. Methods of calculation

The refractive index can be deduced from the equation:

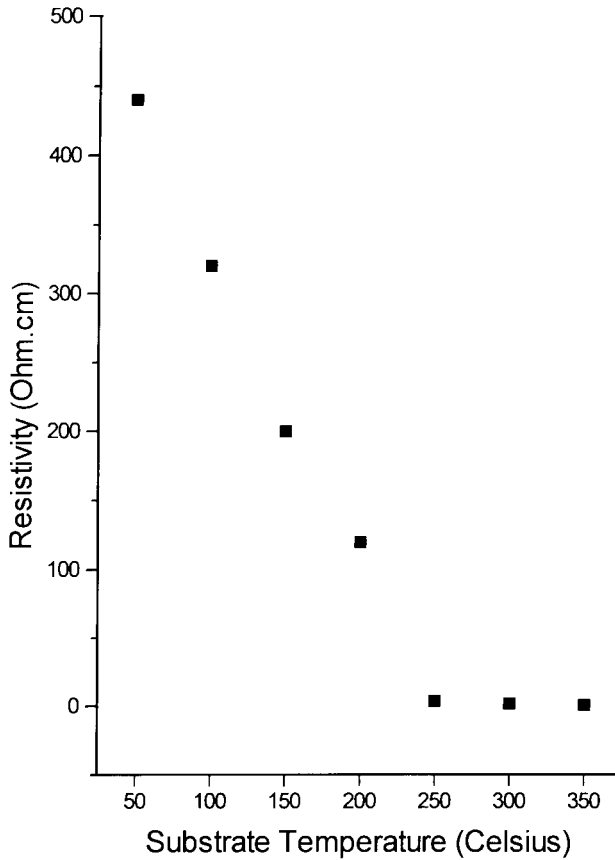


Fig. 3. Resistivity of the SnO<sub>2</sub> films as a function of substrate temperature. R.f. power = 150 W, sputtering time = 1 h, Ar pressure = 25 mtorr.

$$n = \left[ N + (N^2 - n_0^2 n_1^2)^{1/2} \right]^{1/2} \quad (2)$$

where

$$N = (n_0^2 + n_1^2)/2 + 2n_0 n_1 (T_{\max} - T_{\min})/T_{\max} T_{\min} \quad (3)$$

where  $T_{\max}$  and  $T_{\min}$  are the values of asymptotic approached maximum and the minimum of the transmission curve, respectively.

On the other hand in the transparency zone (0.4–0.6  $\mu\text{m}$ ), we can deduce the thickness  $e$  of the specimen by application of the relationship

$$e = M\lambda_1 \lambda_2 / (2[n(\lambda_1)\lambda_2 - n(\lambda_2)\lambda_1]) \quad (4)$$

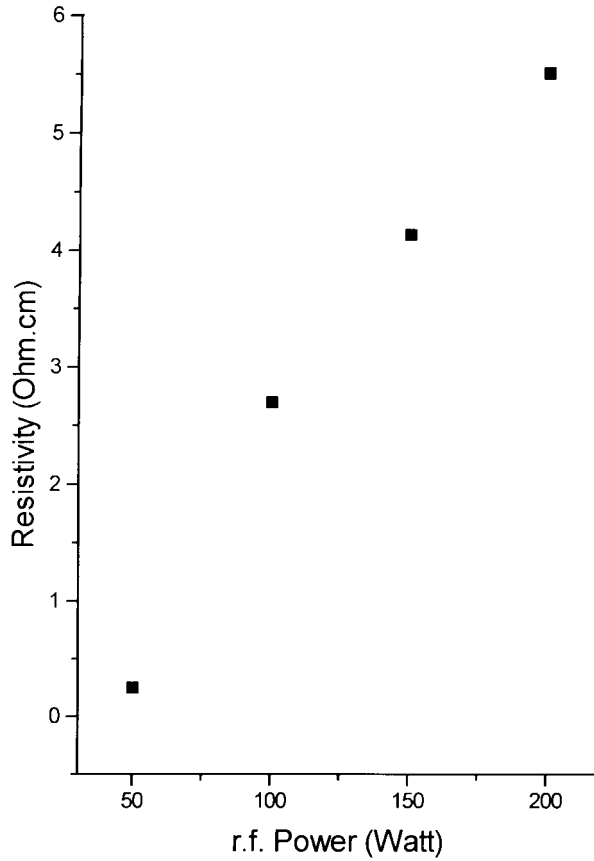


Fig. 4. Resistivity of the  $\text{SnO}_2$  films as a function of r.f.power.  $T_s = 300^\circ\text{C}$ , Air pressure = 25 mtorr.

where  $M$  is the number of oscillations, and  $\lambda_1, \lambda_2, n(\lambda_1), n(\lambda_2)$  are wavelengths and refractive indexes corresponding to two successive extremums.

The average can be calculated from superior and inferior envelopes  $T^+$  ( $T_{\max}$ ) and  $T^-$  ( $T_{\min}$ ) by the relationship of the arithmetic average:

$$T_{\text{ave}} = (T^+ + T^-)/2 \quad (5)$$

### 3.5. Average transmission

A slight increase of the average transmission occurred with the temperature of the substrate when it was increased from 50 to  $200^\circ\text{C}$  (Fig. 5). However, the transmission decreased when the power was raised. The layer exhibited a brownish tint at 150 and 200 W which was attributed to the accumulation of tin.

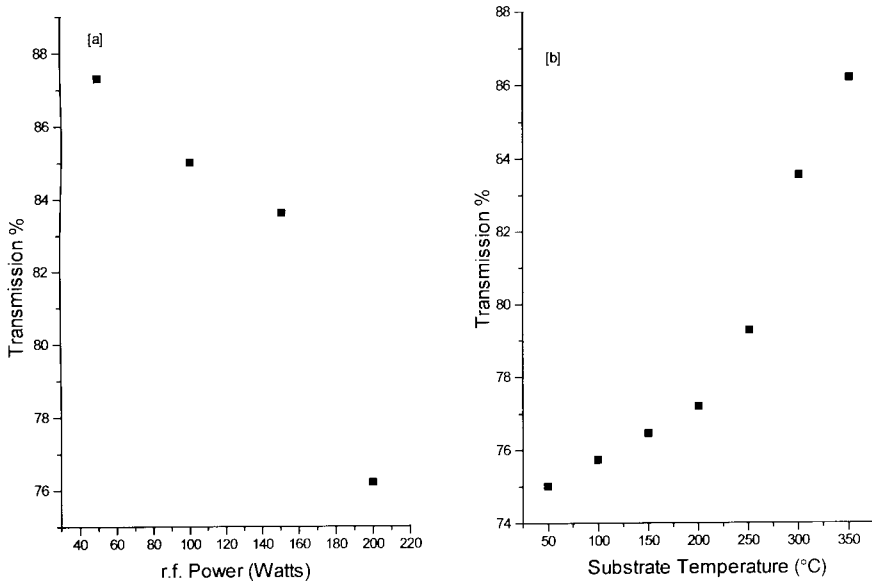


Fig. 5. Dependence of the transmittance on: (a) r.f. sputtering power, (b) the substrate temperature.

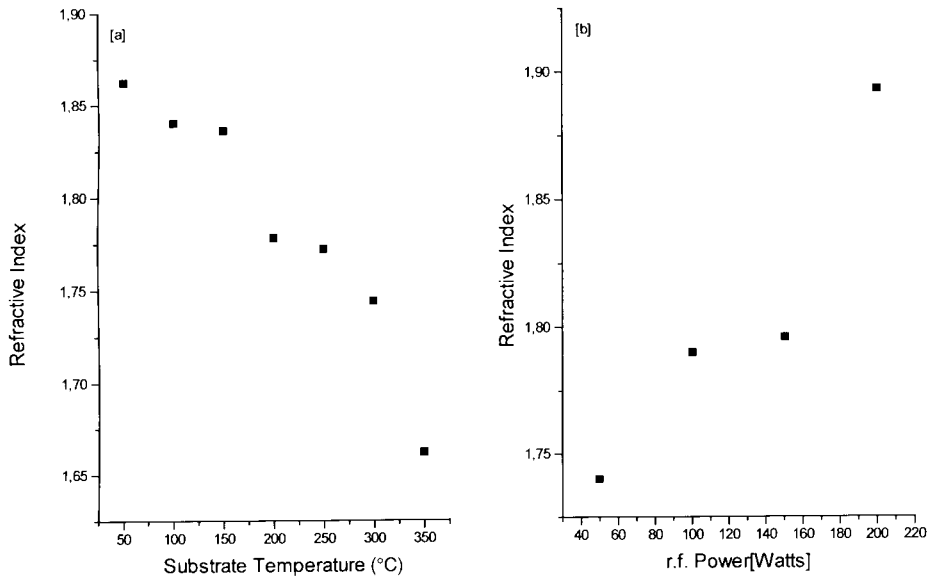


Fig. 6. Refractive index  $n$  versus: (a) r.f. sputtering power, (b) the substrate temperature of the  $\text{SnO}_2$  film.

### 3.6. Refractive index

The refractive index rises with the r.f. power, and diminishes according to the temperature. The best crystallisation was achieved at around 300°C at which the refractive index was approximately 1.7 (Fig. 6).

### 3.7. Absorption coefficient

The coefficient of absorption  $\alpha$  is expressed by the following relation [7]:

$$\alpha = (h\nu - E_g)^\gamma$$

where  $h\nu$  is the radiation energy.

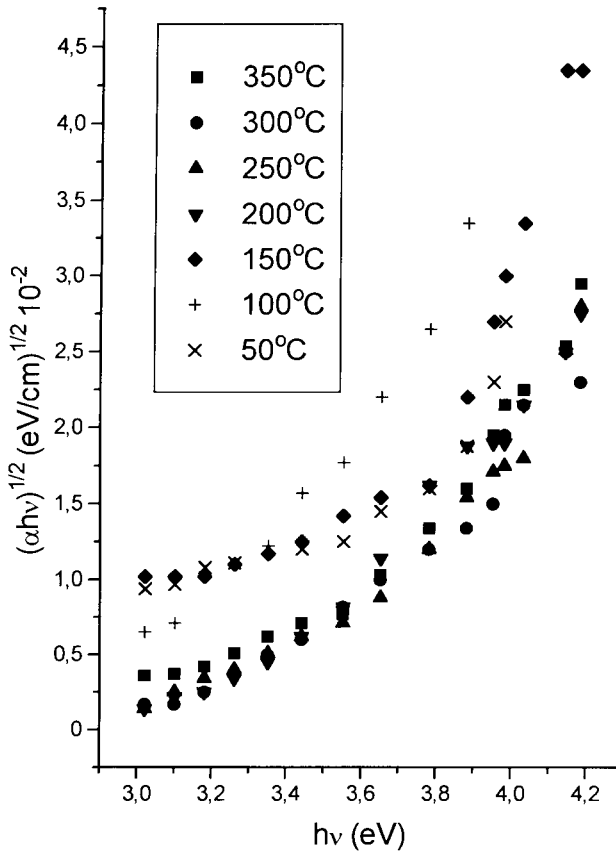


Fig. 7.  $(\alpha h\nu)^{1/2}$  versus the photon energy  $h\nu$  for the tin-oxide films deposited at different substrate temperatures.



$$\text{where } \gamma = \begin{cases} 1/2 & \text{for allowed direct transitions} \\ 3/2 & \text{for forbidden direct transitions} \\ 2 & \text{for forbidden transitions} \end{cases}$$

The variation of the coefficient of absorption according to  $h\nu$  is given by:

$$\alpha = 1/e \ln \frac{\left[ \left( (1 - R_1)^2 (1 - R_2)^2 + 4R_1 R_2 T^2 \right)^{1/2} - (1 - R_1)(1 - R_2) \right]}{2R_1 R_2} \quad (6)$$

where  $e$  and  $T$  are the thickness and the film transmission respectively, and

$$R_1 = (n_1 - n_0)/(n_1 + n_0) \text{ and } R_2 = (n_2 - n_1)/(n_2 + n_1)$$

where  $n_0$  is refractive index of the air which equals unity,  $n_1$  refractive index of the layer, and  $n_2$  the refractive index of the substrate and equals 1.53. Melshmeir et al. [8] have demonstrated that for the polycrystalline structure undoped  $\text{SnO}_2$

$$\alpha h\nu = Cte(h\nu - E_g)^2 \quad (7)$$

On the other hand for  $\text{SnO}_2$  of amorphous structure

$$\alpha h\nu = Cte(h\nu - E_g)^3 \quad (8)$$

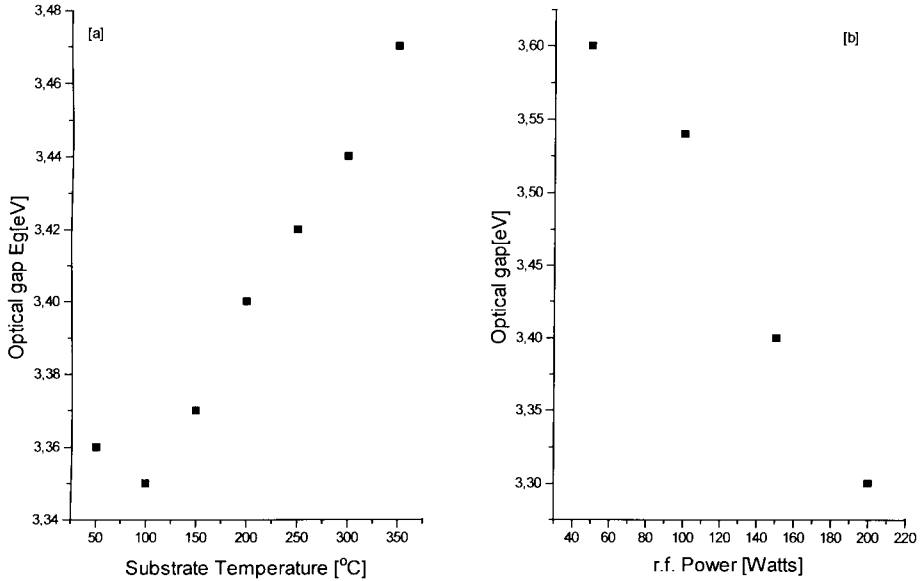


Fig. 8. (a) The optical gap shown as a function of a substrate temperature for tin-oxide films. (b) Optical gap of  $\text{SnO}_2$  as a function of the r.f. power.

where  $E_g = E_c - E_v$  (9)

One can determine therefore the optical gap by the extrapolation of the linear part of  $(\alpha h\nu)^{1/2}$  (Fig. 7) until its intersection with the energy axis.

We observe according to Fig. 8a and b that the direct optical-band-gap varies slightly with the temperature of the substrate, whereas it declines with the r.f. power and increases with the thickness. This is due to the energy-level populations of and the increase of the number of defects.

#### 4. Conclusion

Undoped tin-oxide films were prepared by r.f. sputtering. The films crystallise and grains grow with substrate heating. The electrical resistivity of  $\text{SnO}_{2-x}$  films decreases by orders of magnitude as a result of the substrate. The drop in the resistivity is attributed to the disappearance of the localised electron traps via crystallisation as well as a slow increase of charge-carrier concentration after heating the substrate. The effective band-gap increases from 3.36 eV for the as-deposited tin oxide film, to 3.6 eV for the 300°C heated one. The same reasons are responsible of the transmittance gain of the heated films. The loss of the transmittance with r.f. power can be explained by the introduction of more defects with more energetic deposited atoms.

#### Acknowledgements

This work is supported by the JICA (Japan International Cooperation Agency) office.

#### References

- [1] Manificier JC, De Murcia M, Fillard JP. *Thin Solid Films* 1977;41:127.
- [2] Chopra KL, Major S, Pandaya DK. *Thin Solid Films* 1983;102:1–46.
- [3] Valdes LB. *Proc IRE* 1954;42:420–7.
- [4] Manificier JC, Gassiot J, Fillard JP. *J Phys* 1976;E9:1002.
- [5] Melsheimer J, Ziegler D. *Thin Solid Films* 1985;129:35–47.
- [6] Manificier JC. *Thin Solid Films* 1982;90:219–308.
- [7] Smith RA. *Semiconductors*. 2nd ed. London: Cambridge University Press, 1979.
- [8] Melsheimer J, Tesche B. *Thin Solid Films* 1986;138:71–8.